ELSEVIER

Surface Science 402–404 (1998) 831–835

surface science

Scanning tunneling microscopy observation of surface reconstruction of Si(100) during chemical vapor deposition from Si_2H_6

Deng-Sung Lin *

Institute of Physics, National Chiao-Tung University, 75 Bo-Ai Street, Hsinchu 300, Taiwan

Received 17 July 1997; accepted for publication 5 November 1997

Abstract

This study employs real-time high-temperature scanning tunneling microscopy to examine the evolution of the surface atomic structure of Si(100) during homoepitaxy by chemical vapor deposition at 625°C. At the initial stage, a $(2\times n)$ structure is gradually formed, and the growth mode is pure step flow, followed by double step flow after a single-domain surface is obtained due to faster step advance of S_B than S_A. As growth proceeds, areas with $c(4\times 4)$ symmetry appear, grow, and eventually cover the entire surface.

Keywords: Chemical vapor deposition; Disilane; Scanning tunneling microscopy; Silicon

1. Introduction

The evolution of surface atomic structure during epitaxy is currently receiving extensive and detailed interest [1–8]. Many studies have focused on the homoepitaxy Si(100) surface due to its relevance to integrated circuit technology [2–9]. As is generally known, the clean Si(100) surface exhibits a (2×1) dimer reconstruction after typical preparation of high-temperature annealing and quenching. However, several investigations have noted that rapid thermal quenching [10,11], annealing after Ar^+ bombardment [12], etching (O_2, Br_2, I_2, etc.) [13–15], and homoepitaxy contribute to the formation of the $(2\times n)$ $(6\leq n\leq 12)$ defect structure on Si(100) [4,5]. The $(2\times n)$ reconstruction is formed by regularly spaced dimer vacancy (DV) lines running perpendicular to every nth dimer row. Note that the type of $(2\times n)$ formed during etching and growth contains only Si, and therefore differs significantly from the Ni-induced $(2\times n)$ in many respects as thoroughly discussed by Zandvliet [15].

In addition, a $c(4\times 4)$ structure has been reliably obtained by exposing Si(100)-(2×1) with H followed by annealing between 570 and 690°C among other special treatments [16]. Also, growth of Si epilayers between ~650 and 750°C by both molecular-beam epitaxy (MBE) and chemical vapor deposition (CVD) consistently leads to the formation of the same $c(4\times 4)$ reconstruction [2,4,6] and to the coexistence of the $(2\times n)$ and $c(4\times 4)$ phases [4]. These investigations have verified that the Si(100)-$c(4\times 4)$ surface consists only of Si, and Uhrberg et al. [16] established a mixed ad-dimer structure based on first principle calcula-

* Corresponding author. Fax: (+886) 3-572-0728; e-mail: dslin@cc.nctu.edu.tw

0039-6028/98/$19.00
PII: S0039-6028(97)00894-7

tions. Most recently, a study using real-time variable-temperature scanning tunneling microscopy (VT-STM) showed that annealing the Si(100)-(2×1) surface between 590 and 700°C for hours causes dimer vacancies to increase and nucleate into chains, ultimately forming the $(2\times n)$ structure [17]. The study also showed that $c(4\times4)$ areas appear, grow, and finally cover the entire surface after further annealing the $(2\times n)$ vacancy structure, indicating that the vacancy concentration and its associated strain energy may play a role in driving the $(2\times1)\rightarrow(2\times n)\rightarrow c(4\times4)$ transitions.

In this study, we employ VT-STM to monitor in real time the changes of Si(100) surface structure during Si CVD using a disilane gas source at 625°C. Experimental results demonstrate that the (2×1) surface exhibits increasingly more DV lines in the initial stage, subsequently leading to a $(2\times n)$ phase. As growth proceeds, $c(4\times4)$ domains appear and grow and the surface becomes covered predominantly by the $c(4\times4)$ structure. The structural evolution observed herein in real space and in real time closely corresponds to that obtained by refraction high-energy electron diffraction (RHEED) [2,6].

2. Experimental procedure

STM measurements were taken in a UHV chamber (base pressure $<1\times10^{-10}$ Torr) equipped with a commercial VT-STM system made by Omicron. The Si(100) samples were sliced from 10 Ω cm B-doped wafers. The wafer misalignment is around 0.1° toward ⟨011⟩. Substrate cleaning involved outgassing at ~600°C followed by heating to ~1200°C for a few seconds. Disilane (ultra-high purity grade) was introduced into the chamber through a precision leak valve. The dosing pressure was monitored by an ionization gauge which did not directly face the sample. The pressure readings of the ion gauge were corrected by the gauge's sensitivity to Si_2H_6, which is around 2.4 relative to air [8]. The sample was annealed by passing a current through it, and the temperature of the samples was measured with an infrared pyrometer.

3. Results and discussion

Fig. 1a, taken at room temperature, depicts a 4000×2000 Å^2 STM image of the initially clean Si(100)-(2×1) surface with a low concentration of DVs. At this scale, individual atoms and dimers cannot be seen. The primary features in Fig. 1a denote alternatively smoother and rougher steps (so-called S_A and S_B, respectively). Each step separates two degenerate reconstruction terraces (T_A and T_B) with their dimer rows running parallel (perpendicular) to the domain edges. After the sample is heated and maintained at 625°C for about 1 h, the thermal drift becomes sufficiently small for imaging. As Fig. 1b depicts, the basic step structure of S_A and S_B remains largely the same. The step edges appear hairy due to thermal-induced fluctuations at this temperature. On the terraces, DVs and DV lines, signaled by dark spots and short lines, evenly disperse on the surface. These DVs are thermally generated [17]. At this temperature, DVs are adequately able to move around, leading to individual DVs being nucleated into short chains running perpendicular to the dimer rows. The ordering of DVs is driven by the DV–DV interaction [11,15].

Fig. 1c–h illustrates the UHV–CVD homoepitaxial growth experiment. In this study, the surface of Fig. 1b was exposed to disilane ($\sim1\times10^{-8}$ Torr) for 6.6, 16.2, 28.2, 39.6, 82.2, and 207 L (1 L = 10^{-6} Ts) for Fig. 1c–h, respectively, while being maintained at 625°C. The initial growth rate is estimated to be approximately 0.055 ML/L. The reactive sticking probability of disilane is therefore around 0.05, in close agreement with that deduced from time-of-flight direct recoiling measurement [9]. At this temperature, H desorbs upon adsorption of disilane fragmentation, and its surface coverage is near zero since the H desorption temperature (~500°C) is well below the growth temperature. The adsorbed Si adatoms left behind after H desorption are sufficiently mobile to reach the step edges, leading to step-flow growth, as Fig. 1c–e reveals. As concluded by several previous investigations [3], the adatom incorporation rate into S_B steps is markedly higher than that of S_A steps, leading to faster advance of S_B steps and the formation of nearly

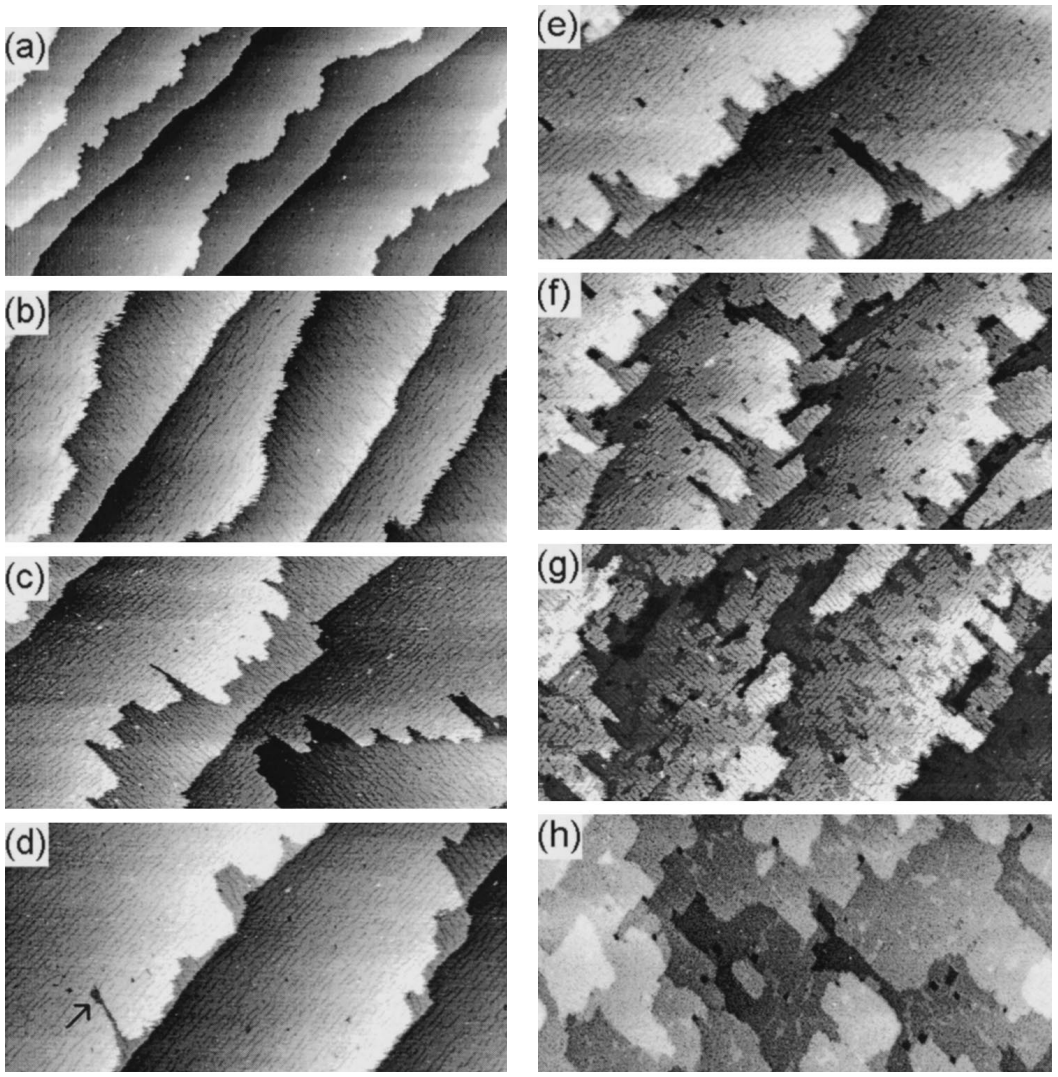

Fig. 1. (a) STM images of the starting Si(100)-(2×1) surface taken at RT. (b–h) Images obtained in real time after the Si(100) surface is maintained at 625°C and exposed to 0, 6.6, 16.2, 28.2, 39.6, 82.2, and 207 L of disilane, respectively. The tip bias (V_t) was 2.0 V. The image sizes are 4000×2000 Å^2.

single-domain surfaces, as Fig. 1d depicts. During the growth of the first monolayer, the DV lines continue developing evenly on the terraces and, ultimately, form a $(2\times n)$ ($n\sim11$ in Fig. 1d) structure. As Fig. 1d reveals, a few voids exist of a monolayer deep. As illustrated by a developing void identified by an arrow, the voids result from step pinning at defects. As the disilane dosage increases, the surface remains largely single domain, and the growth proceeds by a double step flow. This growth behavior resembles that observed during MBE at a lower temperature (~500°C) [3,5]. In addition to the darkish monolayer-deep voids, there appears another type of patch scattered on the surface in Fig. 1f. As shown in a close-up filled state image (Fig. 2), these patches comprise characteristic bright features which locally form a square pattern showing the $c(4\times4)$ periodicity [4,16]. The $c(4\times4)$ domains in the middle of a terrace are in the same atomic

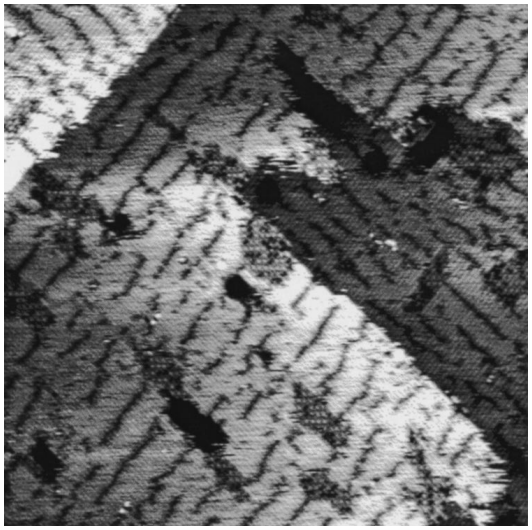

Fig. 2. Close-up image ($\sim 1000 \times 800$ Å^2) showing patches of the $c(4\times4)$ domains. The image was acquired between Fig. 1f and g with $V_t = 2$ V.

layer with their surrounding $(2\times n)$ areas, but appear darker in Fig. 1f and g due to both electronic and topological effects [4]. Notably, the $c(4\times4)$ structure shows a strong tendency to condense around S_B steps, as shown in Fig. 2. Also, Fig. 1f reveals that the population of T_A terraces increases and the growth deviates from the double-layer growth mode. Such behavior can be rationalized by assuming that the $c(4\times4)$ domains condensed around the S_B steps reduce the anisotropy of adatom accommodation probabilities on the alternative steps. As the exposure further increases, the $c(4\times4)$ continue growing and finally cover the entire surface, as Fig. 1g and h depicts.

In the RHEED study of the identical growth system by Liu et al. [2] in the similar growth temperature range, a disordered (2×1) pattern formed initially. The splitting and lengthening of the diffraction streaks, rising from one-dimensional disorder boundaries, corresponds well to the formation of DV lines in the $(2\times n)$ structure seen in Fig. 1. With increasing Si coverage, features of the $c(4\times4)$ RHEED pattern started to emerge and became sharper and more intense, indicating that the surface became covered predominantly by $c(4\times4)$ domains. The growth rate (20 Å/min) employed in ref. [2] is 1000 times faster than that in this study. Yet, the same structure transition to $c(4\times4)$ is observed even though a slower growth rate allows the crystal time to attain minimization of free energy. Nayak et al. [6] also reported similar RHEED results using silane. Therefore, our real-space observation of the surface structure during the Si CVD growth processes correlates well with that found by the traditional diffraction method. The surface reconstruction evolves from (2×1) to $(2\times n)$, then to $c(4\times4)$. In addition, Fig. 1g resembles the images obtained on annealed Si MBE homoepitaxial layers, showing the coexistence of $(2\times n)$ and $c(4\times4)$ [4]. Notably, the structural evolution in Fig. 1 strikingly resembles that found during extensive annealing of the Si(100) surface itself, even though no external gas is involved. If annealing the Si(100)-(2×1) surface results in the $(2\times1)\rightarrow(2\times n)\rightarrow c(4\times4)$ transformation at low temperatures as Ref. [17] showed, the structure evolution observed herein for the CVD growth therefore may not directly originate from the growth itself. This is further evident because the formation of $(2\times n)$ and $c(4\times4)$ domains does not follow the growth fronts (steps). The fact that the time to convert the entire surface into $c(4\times4)$ during the growth is much shorter than that during annealing at the same temperature leads us to infer that the hydrides play an influential role in enhancing the structure transformation, since the structural transformation time can be shortened by increasing the disilane flow rate [2].

Acknowledgements

This work is supported by the National Science Council, Republic of China on Taiwan, under Contract No. NSC86-2613-M009-001.

References

[1] I. Goldfard, P.T. Hayden, J.P. Hayden, J.H.G. Owen, G.A.D. Briggs, Phys. Rev. Lett. 78 (1997) 3959.
[2] W.K. Liu, S.M. Mokler, N. Ohtani, B.A. Joyce, Surf. Sci. 264 (1992) 301.

[3] B. Voigtlander, T. Weber, P. Smilauer, D.E. Wolf, Phys. Rev. Lett. 78 (1997) 2164.
[4] Z. Zhang, M.A. Kulakov, B. Bullemer, Surf. Sci. 369 (1996) 69.
[5] A.J. Van Hoven, D. Dÿkkamp, E.J. van Loenen, J.M. Lenssinck, J. Dieleman, J. Vac. Sci. Technol. A8 (1990) 207.
[6] S. Nayak, D.E. Savage, H.-N. Chu, M.G. Lagally, T.F. Kuech, J. Crystal Growth 157 (1995) 168.
[7] M.J. Bronikowski, Y.-W. Wang, M.T. McEllistrem, D. Chen, R.J. Hamers, Surf. Sci. 298 (1993) 50.
[8] D.-S. Lin, T. Miller, T.-C. Chiang, J. Vac. Sci. Technol. A15 (1997) 919.
[9] S.M. Gates, S.K. Kulkarni, Appl. Phys. Lett. 60 (1992) 53.
[10] J.A. Martin, D.E. Savage, W. Moritz, M.G. Lagally, Phys. Rev. Lett. 56 (1986) 1936.
[11] F.K. Men, A.R. Smith, K.J. Chao, Z. Zhang, C.K. Shih, Phys. Rev. B 52 (1995) R8650.
[12] H. Feil, Phys. Rev. Lett. 69 (1992) 3076.
[13] K.E. Johnson, P.K. Wu, M. Sander, T. Engel, Surf. Sci. 290 (1993) 213.
[14] Y. Wei, Y. Hong, I.S.T. Tsong, Appl. Surf. Sci. 92 (1996) 491.
[15] H.J.W. Zandvliet, Surf. Sci. 377–379 (1997) 1.
[16] R.I.G. Uhrberg, J.E. Northrup, D.K. Biegelsen, R.D. Brigans, L.E. Swartz, Phys. Rev. B 46 (1992) 10251, and references cited therein.
[17] D.S. Lin, P.H. Wu, Surf. Sci. 397 (1998) L273.